CRACK SHAPE STUDY IN A BRITTLE, NON-BONDED, PARTICULAR COMPOSITE

D. J. Green, P. S. Nicholson and J. D. Embury*

INTRODUCTION

The interaction of the crack front with obstacles [1-3] may produce changes in crack shape which have an important influence on the fracture of brittle materials. Lange [1] postulated that a crack front may possess a line tension in analogy with dislocation theory. This hypothesis would seem rather tenuous as there is a difference in the range of the stress fields of these two defects and the difficulty of defining the displacement vector for the crack. Evans [2] has produced an alternative treatment to calculate the increase in elastic strain energy associated with various crack shape configurations. This work indicates that pinning of a crack front by impenetrable obstacles could lead to an increase in fracture toughness under some circumstances.

The evidence for changes in crack shape in the vicinity of second-phase obstacles has been mainly derived from fractographic observations. More recently, the technique of ultrasonic fractography has been used for a study of crack shape in a porous glass [4]. In this technique, a beam of transverse ultrasonic waves is used to modulate the path of a growing crack so that it leaves a permanent ripple marking on the fracture surface. This elegant technique was originally developed by Kerkhof and his co-workers [5] for crack speed studies. The crack velocity is simply determined from the spacing of the ripple markings which are imprinted at a known frequency.

In this work, a study was made of the variation in crack shape and fracture toughness of a non-bonded, nickel sphere-glass matrix composite. This sytem should act as a lower limiting case of increased toughness because the nickel spheres should act more like voids which do not pin the crack but act instead to locally blunt the crack front and impede its motion.

EXPERIMENTAL

A series of S glass[1]-nickel sphere[2] composites were produced by vacuum hot-pressing appropriate glass powder-nickel mixtures at 700°C for 10 to 15 minutes [6]. The hot-pressed billets were then annealed at 450°C to remove any internal stresses that result from the fabrication procedure. The billets were then diamond-machined into DCB fracture samples with approximate dimensions 50mm x 12mm x 6mm. The samples were side-grooved to a depth of 2mm and notched. Machining stresses were removed by a

*McMaster University, Hamilton, Ontario, Canada.
D. J. Green now at Canada Centre for Mineral and Energy Technology, Ottawa, Canada.

[1]S glass (55 wt % SiO_2, 15 wt % Al_2O_3, 30 wt % Na_2O)

[2]Average size 132 μm. Sherritt-Gordon Mines Ltd., Toronto, Canada.

second anneal at 450°C. The final step in the machining procedure was to pre-crack the samples. This operation was monitored by an audible "click" as the pre-crack was formed and grown.

One series of samples was used to measure the value of G_{IC} as a function of the volume fraction of nickel (to 20 vol.%). These values were determined from load and displacement measurements using an Instron testing machine and extensometer [6]. For the second series of samples, an ultrasonic transducer was glued to the end of the sample opposite the notch. The frequency of the ultrasonic waves was 1.02MHz and a 1kW transmitter was used to drive the crystal.

Fractographic observations were made on the ultrasonically-modulated samples using the SEM and Nomarski interference microscopy. Before describing the experimental results it is of value to consider a simple theoretical model to describe crack particle interactions.

Evans [2] has compared the stress to move semi-circular secondary cracks (σ_a^s) between a row of impenetrable obstacles with the stress to move the primary crack (σ_c) of length C'. The model assumes semi-circular segments of radius C separated by particles of radius r_o and that the crack origin is pushed forward from the planar position a distance r between the obstacles. In his work, Evans used approximate analytical solutions for large and small values of C/r and numerical solutions for the intermediate values. This calculation was repeated using numerical integration for all values of C/r and the results are shown for C'>>C in Figure 1. The amount of pinning and the value of σ_a^s/σ_c depends on the value of r. For impenetrable obstacles Evans took $r = 2r_o$ i.e. breakaway occurs when the secondary cracks reach the rear of the particle. For the case of crack front interaction with a void [4] it was seen that although the crack front was impeded by the presence of the void, the crack is not pinned in the sense that r = 0. For this limiting case we have $\sigma_a^s/\sigma_c = 1.30$.

It is clear that these secondary cracks need not be semi-circular and by converting to semi-elliptical conditions, Evans [2] was able to predict the crack shape at breakaway and the value of σ_a^e/σ_c where σ_a^e is the stress needed to move the semi-elliptical secondary cracks.

However, a numerical solution of the problem indicated some additional points of interest. It was found that the ratio of the minor to major axes of the secondary elliptical cracks (a/c) would not be greater than unity. In this sense, a semi-elliptical crack would tend towards semi-circular conditions especially for small values of C but would never exceed it. This result is more consistent with the expected behaviour of an elliptical crack [7]. Secondly, it was found that the value of σ_a^e/σ_c is approximately unity for large values of C/r or for the case where r = 0. This result would also appear more logical since one would expect no increase in the stress ratio for infinitely-spaced obstacles. The stress ratio σ_a^e/σ_c is shown in Figure 2 for the situation where $r = r_o$. Finally, it was found that larger values of σ_a^e/σ_c could be obtained than those predicted by Evans [2].

Thus as an extension of Evans's analysis, it can be concluded that for the case of a crack interacting with a void and hence r = 0, the value of $\sigma_a^e/\sigma_c = 1$ and the crack should not change shape [4,6].

RESULTS AND DISCUSSION

The results of the fracture toughness testing are shown in Figure 3 and it can be seen that there is an increase in G_{IC} as the volume fraction of nickel is increased. These values were corrected to account for the decrease in fracture surface area as the volume fraction of nickel is increased. For a non-bonding situation the nickel spheres should make no contribution to the fracture surface area. Figure 4 shows a typical micrograph for an ultrasonically-modulated surface. It can be seen that the crack is not pinned by the sphere but there is a change in crack shape as the crack segments to bypass the obstacle. Finally, as the crack breaks away from the sphere, the segmented secondary cracks have also changed plane and a fracture surface step has to be formed at the rear of the particle. This behaviour is very similar to that observed for the S glass-pore system [4] but is not in accord with the simple theoretical model described above.

From the ultrasonic samples, fractographic observations were used to determine the crack shape at breakaway. This was done by approximately the secondary crack to a semi-ellipse and measuring a/2C at breakaway. The result of these measurements are shown in Figure 5 along with the theoretical shape predicted from the re-analysis of Evans' work [2]. There is considerable scatter in the data but there is a tendency for an increase in a/2C as the interplanar spacing decreases. The stress to move these semi-elliptical cracks can be estimated by using the elliptical flaw shape parameter [2]: $\sigma_a^e/\sigma_c^s = Z$. For the case of no pinning $\sigma_a^s/\sigma_c = 1.30$ and we evaluate σ_a^e/σ_c for the particular crack shape variation observed. This result is shown in Figure 6 and it can be seen from these elastic strain energy considerations that the change in crack shape should lead to no increase in σ_a^e/σ_c and hence G_{IC}.

The change in crack shape in accord with the theory must therefore arise due to factors not considered in the original model. For example, the stress state at the particle interface must correspond to plane stress as the non-bonded interface will act as a free surface. For positions between the obstacles, the stress state must be plane strain or some intermediate state. For a highly brittle material, the difference between the plane stress and plane strain values of G should just be a result of the $(1-\mu^2)$ factor, which for this system should be about a 6% correction. There are other mechanisms which will play a role in the fracture of these composites. Surface roughness and the production of the fracture surface steps will lead to an increased fracture surface area compared to that expected from planar extension. Fractographic observations of these features, however, indicate that the increase in surface area is probably less than 30%. It is also clear that the nickel spheres will act to locally blunt the crack tip and thereby decrease the stress concentration at the crack tip. In this sense it is clear that the particles impede the crack front by the local decrease in elastic strain energy. This blunting problem has been analysed by Berry[8] but he shows that this effect will only make a negligible correction to an energy criterion for fracture provided the crack tip radius is small compared to the crack length, a criterion that is satisfied for the fracture toughness tests.

However, the local blunting of the crack front and the associated decrease in the stress concentrations near the obstacle makes it necessary to overstress the secondary cracks as they bypass the obstacles. This over-

stressing gives rise to the high observed crack velocity as the cracks break away from the spheres and an increase in G_{IC} [6].

ACKNOWLEDGEMENTS

This work was sponsored by the Atomic Energy of Canada Ltd. The authors would like to acknowledge important discussions with R. G. Hoagland, F. Kerkhof and M. G. Schinker.

REFERENCES

1. LANGE, F. F., Phil. Mag., 22, 1970, 983.
2. EVANS, A. G., Phil. Mag., 26, 1972, 1327.
3. EVANS, A. G. and GRAHAM, L. J., Acta Met., 23, 1975, 1303.
4. GREEN, D. J., NICHOLSON, P. S., EMBURY, J. D., submitted to J. Mat. Sci., 1976.
5. KERKHOF, F., Bruchvorgängen in Gläsern, Verlag der Deut. Glastech. Ges., Frankfurt, 1970.
6. GREEN, D. J., Ph.D. Thesis, McMaster University, 1976.
7. IRWIN, G. R., J. Appl. Mech., 24, 1957, 361.
8. BERRY, J. P., Fracture Processes in Polymeric Solids, ed. B. Rosen, p.172, J. Wiley and Sons, New York, 1964.

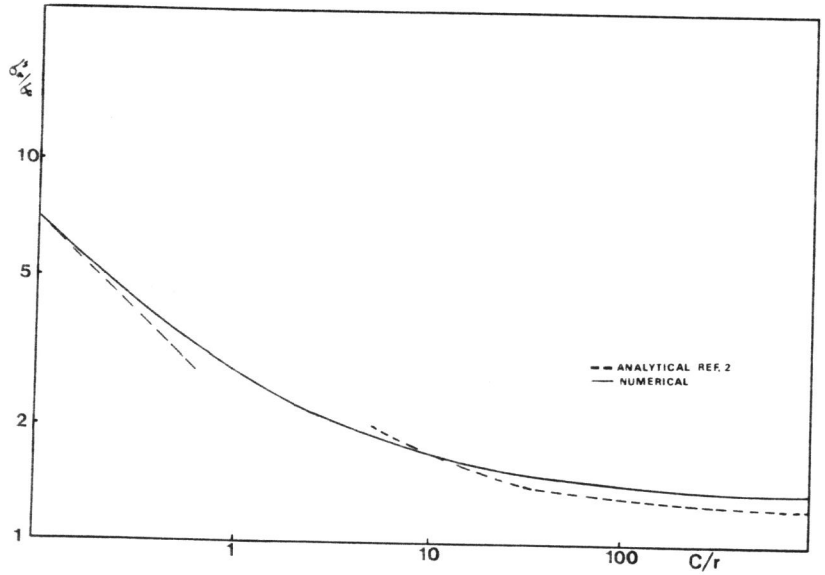

Figure 1 Ratio of Stress to Move Semi-Circular Secondary Cracks to Stress to Move Primary Crack

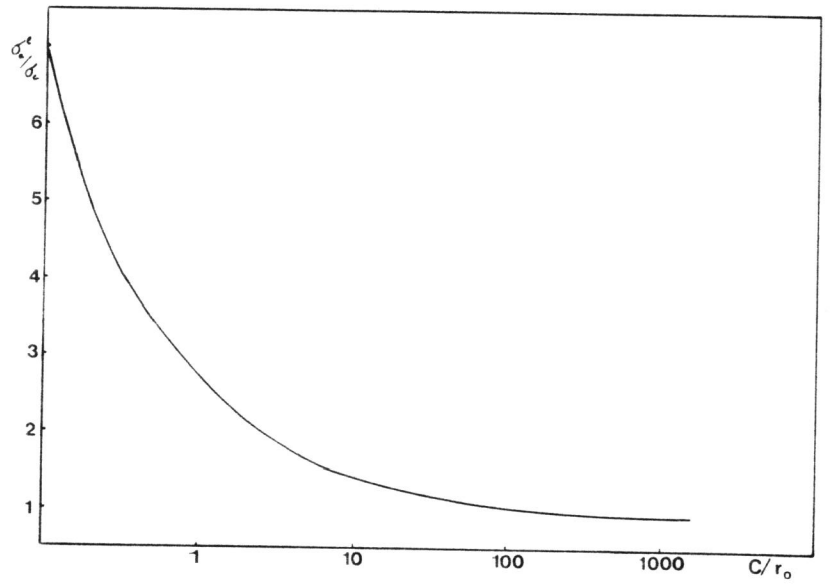

Figure 2 The Stress Ratio σ_a^e/σ_c as a Function of C/r_o for the Breakaway Position $r = r_o$

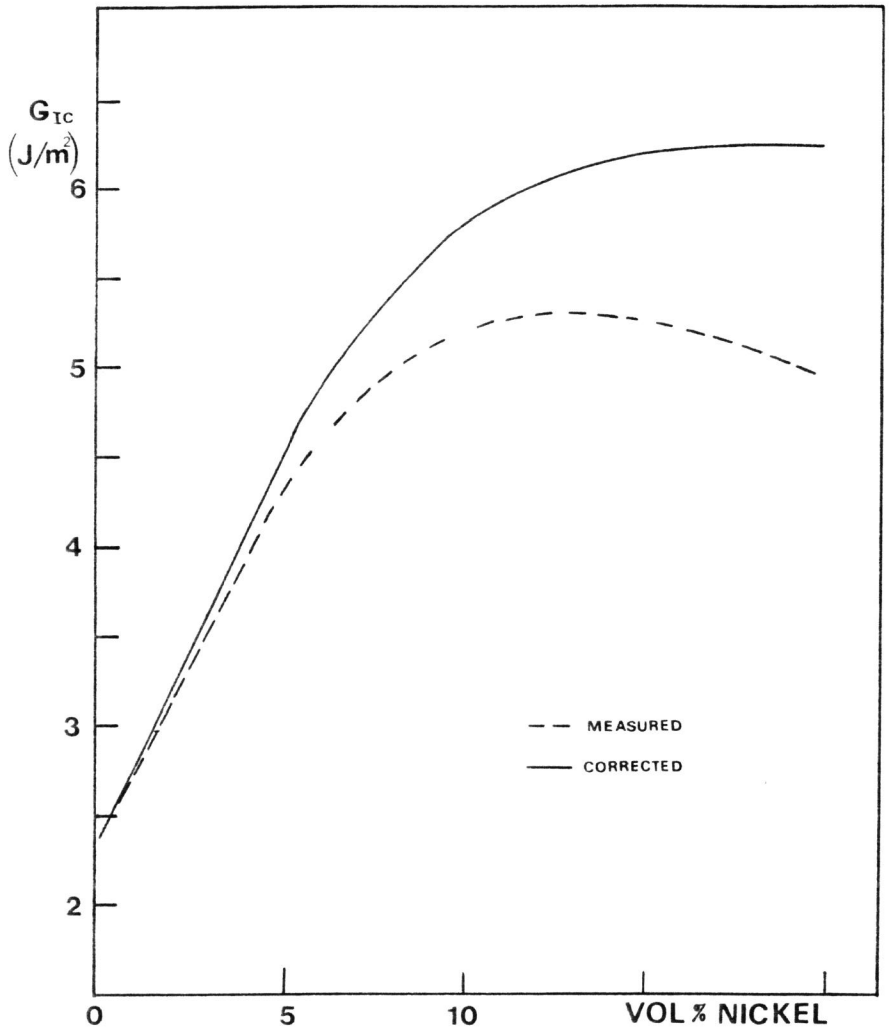

Figure 3 Critical Strain Energy Release Rate G_{IC} as a Function of Volume Fraction of Nickel Spheres

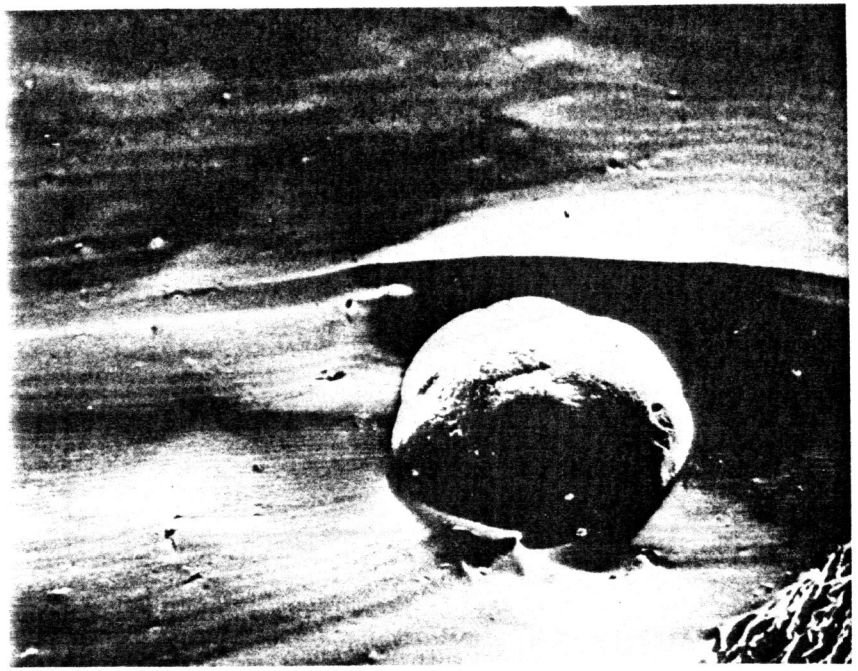

Figure 4 SEM Micrograph of Ultrasonically-Modulated Surface (Mag. 400X)

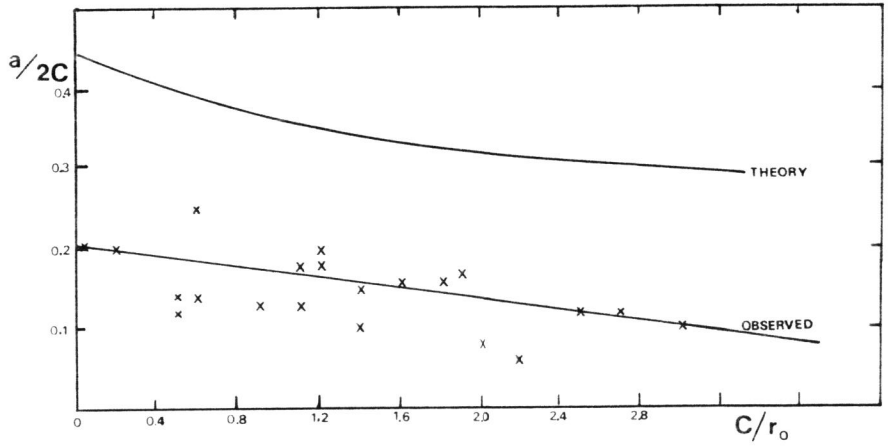

Figure 5 Semi-Elliptical Flaw Shape at Breakaway

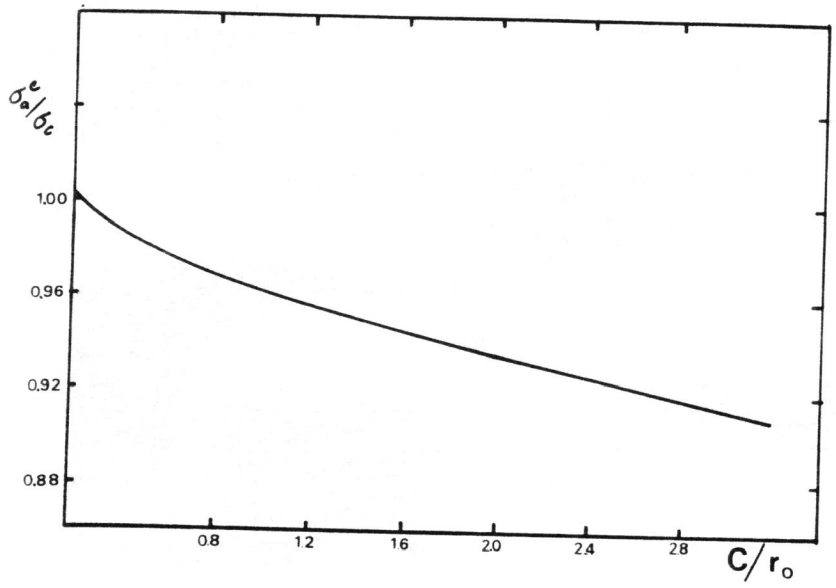

Figure 6 The Stress Ratio σ_a^e/σ_c Based on Fractographic Observations